J|A|C|S
ARTICLES

Published on Web 07/13/2010

Exploiting Enzymatic Promiscuity to Engineer a Focused Library of Highly Selective Antifungal and Antiproliferative Aureothin Analogues

Martina Werneburg,[†] Benjamin Busch,[†] Jing He,[†] Martin E.A. Richter,[†] Longkuan Xiang,[§] Bradley S. Moore,[§] Martin Roth,[†] Hans-Martin Dahse,[†] and Christian Hertweck*[,†,‡]

Leibniz Institute for Natural Product Research and Infection Biology, HKI, Dept. of Biomolecular Chemistry, Beutenbergstr. 11a, 07745 Jena, Germany, the Friedrich Schiller University, Jena, Germany, and the Scripps Institution of Oceanography and Skaggs School of Pharmacy and Pharmaceutical Sciences, University of California at San Diego, La Jolla, California, 92093-0204

Received April 1, 2010; E-mail: christian.hertweck@hki-jena.de

Abstract: Aureothin is a shikimate-polyketide hybrid metabolite from *Streptomyces thioluteus* with a rare nitroaryl moiety, a chiral tetrahydrofuran ring, and an *O*-methylated pyrone ring. The antimicrobial and antitumor activities of aureothin have caught our interest in modulating its structure as well as its bioactivity profile. In an integrated approach using mutasynthesis, biotransformation, and combinatorial biosynthesis, a defined library of aureothin analogues was generated. The promiscuity of the polyketide synthase assembly line toward different starter units and the plasticity of the pyrone and tetrahydrofuran ring formation were exploited. A selection of 15 new aureothin analogues with modifications at the aryl residue, the pyrone ring, and the oxygenated backbone was produced on a preparative scale and fully characterized. Remarkably, various new aureothin derivatives are less cytotoxic than aureothin but have improved antiproliferative activities. Furthermore, we found that the THF ring is crucial for the remarkably selective activity of aureothin analogues against certain pathogenic fungi.

Introduction

Natural products are known to represent the major source for novel therapeutics, in particular in the field of antiinfectives and antitumoral agents.[1,2] This is not surprising in light of the hypothesis that many of these compounds contribute toward defending the producer's ecological niche and have undergone evolutionary selection and optimization.[3,4] Nonetheless, natural products as such are not necessarily suited as therapeutics. To reduce undesired side effects, improve bioavailability issues, and modulate their bioactivity profile, natural products typically undergo a chemical post-evolution through semisynthesis (i.e., derivatization) or total synthesis of analogues prior to clinical trials.[5,6] During the past two decades, the portfolio of methods for structural variation has been greatly increased by the knowledge of biosynthetic pathways and their rational reprogramming. Synthetic methods can now be complemented by feeding synthetic building blocks to suitable mutant strains (mutasynthesis),[7,8] using individual enzymes for biotransformations,[9] and swapping biosynthesis genes in a mix-and-match fashion (combinatorial biosynthesis).[10−12] These techniques have been predominantly applied to the large and diverse group of

[†] HKI.
[§] University of California at San Diego.
[‡] Friedrich Schiller University.

(1) Newman, D. J.; Cragg, G. M. *J. Nat. Prod.* **2007**, *70*, 461–477.
(2) Cragg, G. M.; Grothaus, P. G.; Newman, D. J. *Chem. Rev.* **2009**, *109*, 3012–3043.
(3) Osada, H.; Hertweck, C. *Curr. Opin. Chem. Biol.* **2009**, *13*, 133–134.
(4) John, J. E. *Drug Discovery Today* 2010. epub ahead of print, DOI:, 10.1016/j.drudis.2010.02.008.
(5) Newman, D. J.; Cragg, G. M.; Snader, K. M. *Nat. Prod. Rep.* **2000**, *17*, 215–234.
(6) von Nussbaum, F.; Brands, M.; Hinzen, B.; Weigand, S.; Häbich, D. *Angew. Chem., Int. Ed.* **2006**, *45*, 5072–5129.
(7) Weist, S.; Süssmuth, R. D. *Appl. Microbiol. Biotechnol.* **2005**, *68*, 141–150.
(8) Recent examples include the following. Enterocin: Kalaitzis, J. A.; Izumikawa, M.; Xiang, L.; Hertweck, C.; Moore, B. S. *J. Am. Chem. Soc.* **2003**, *125*, 9290–9291. Rapamycin: Gregory, M. A.; Petkovic, H.; Lill, R. E.; Moss, S. J.; Wilkinson, B.; Gaisser, S.; Leadlay, P. F.; Sheridan, R. M. *Angew. Chem., Int. Ed.* **2005**, *44*, 4757–4760. Borrelidin: Moss, S. J.; Carletti, I.; Olano, C.; Sheridan, R. M.; Ward, M.; Math, V.; Nur, E. A. M.; Brana, A. F.; Zhang, M. Q.; Leadlay, P. F.; Mendez, C.; Salas, J. A.; Wilkinson, B. *Chem. Commun.* **2006**, 2341–2343. Ansamitocin: Taft, F.; Brünjes, M.; Floss, H. G.; Czempinski, N.; Grond, S.; Sasse, F.; Kirschning, A. *ChemBioChem* **2008**, *9*, 1057–1060. Geldanamycin: Kim, W.; Lee, J. S.; Lee, D.; Cai, X. F.; Shin, J. C.; Lee, K.; Lee, C. H.; Ryu, S.; Paik, S. G.; Lee, J. J.; Hong, Y. S. *ChemBioChem* **2007**, *8*, 1491–1494. Eichner, S.; Floss, H. G.; Sasse, F.; Kirschning, A. *ChemBioChem* **2009**, *10*, 1801–1805. Myxalamid: Bode, H. B.; Meiser, P.; Klefisch, T.; Cortina, N. S.; Krug, D.; Göhring, A.; Schwär, G.; Mahmud, T.; Elnakady, Y. A.; Müller, R. *ChemBioChem* **2007**, *8*, 2139–2144. Pikromycin: Gupta, S.; Lakshmanan, V.; Kim, B. S.; Fecik, R.; Reynolds, K. A. *ChemBioChem* **2008**, *9*, 1609–1616. Spinosyn: Sheehan, L. S.; Lill, R. E.; Wilkinson, B.; Sheridan, R. M.; Vousden, W. A.; Kaja, A. L.; Crouse, G. D.; Gifford, J.; Graupner, P. R.; Karr, L.; Lewer, P.; Sparks, T. C.; Leadlay, P. F.; Waldron, C.; Martin, C. J. *J. Nat. Prod.* **2006**, *69*, 1702–1710. Salinosporamide: Eustáquio, A. S.; Moore, B. S. *Angew. Chem., Int. Ed.* **2008**, *47*, 3936–3938. Nett, M.; Gulder, T. A.; Kale, A. J.; Hughes, C. C.; Moore, B. S. *J. Med. Chem.* **2009**, *52*, 6163–6167. Liu, Y.; Hazzard, C.; Eustáquio, A. S.; Reynolds, K. A.; Moore, B. S. *J. Am. Chem. Soc.* **2009**, *131*, 10376–10377.
(9) Müller, M. *Curr. Opin. Biotechnol.* **2004**, *15*, 591–598.
(10) Floss, H. G. *J. Biotechnol.* **2006**, *124*, 242–257.

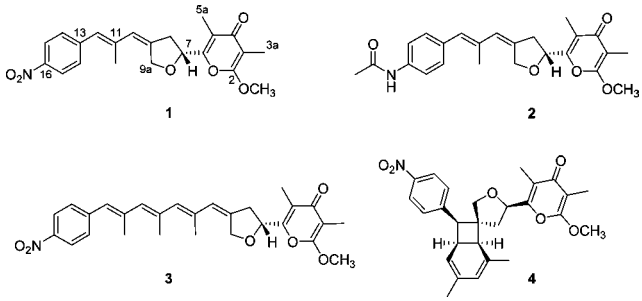

Figure 1. Structures of aureothin (**1**), *N*-acetylaureothamine (**2**), neoaureothin (spectinabilin, **3**), and SNF4435C (**4**).

polyketide metabolites,[13] mainly macrolide antibiotics.[14−18] Yet in comparison, polyketide-derived pyrone compounds, which are considered as a privileged group of bioactive natural products,[19−21] have been less thoroughly investigated to date. The densely functionalized shikimate-polyketide hybrid metabolite aureothin (**1**) is the prototype of a series of related pyrone compounds from actinomycetes. Whereas aureothin (**1**) is known as a cytotoxic agent from the soil bacterium *Streptomyces thioluteus*,[22] *N*-acetylaureothamine (**2**) and neoaureothin (spectinabilin, **3**) were identified because of their potent anti-*Helicobacter*[23] and antiviral activities, respectively.[24] SNF4435C (**4**) and D are known as immunosuppressants[25] derived from neoaureothin by a photoinduced electrocyclic rearrangement[26] (Figure 1). To gain an insight into the biological assembly lines involved in the formation of these metabolites and to harness the biosynthetic potential for the generation of novel analogues, we previously cloned and sequenced the *aur* and *nor* biosynthesis gene loci.[27,28] Here, we report an integrated approach using the combination of mutasynthesis, biotransformation, and combinatorial biosynthesis for the generation of a focused library of aureothin analogues with remarkably selective antifungal and antiproliferative activities.

Results and Discussion

Levels of Diversification in the Enzymatic Aureothin Assembly Line. According to our previous functional analyses, the aureothin biosynthetic pathway is initiated by the formation of *p*-aminobenzoate (PABA) and its subsequent transformation into *p*-nitrobenzoate (PNBA) by a novel nitro group forming *N*-oxygenase (AurF).[29−31] PNBA is then activated by the acyl-CoA ligase AurE and loaded onto the first module of a non-colinear modular type I polyketide synthase (AurA-C), which catalyzes five elongation cycles (Figure 2).[32] After off-loading of the pentaketide with lactonization, the resulting pyrone ring is methylated by AurI,[33] and finally the cytochrome P450 monooxygenase AurH introduces the tetrahydrofuran ring.[34,35] The pathway thus exhibits three general levels that could be envisaged for diversification: incorporation of the starter unit building block,[36] formation of the polyketide backbone, and enzymatic tailoring (i.e., alkylation and oxidative heterocyclization). As initial attempts to alter the aureothin polyketide synthase failed (data not shown), we concluded that the thiotemplate itself is not readily amenable to manipulations. In contrast, mutational analyses of the *aur* gene cluster suggested that both the choice of starter unit and post-PKS tailoring reactions would in principle leave some room for genetically engineering structural variants. While an *aurF* null mutant could be used for mutasynthesis approaches, variants lacking *aurH* or *aurI* would result in deoxy-/hydroxyl- or desmethylaureothin derivatives, respectively. Considering *x* possible starter units, three variants in backbone functionalization (methylene, hydroxyl, tetrahydrofuran), and three different pyrone rings (nonmethylated, α-methlyated, γ-methylated), at least in principle 9 *x* aureothin derivatives could be generated.

Tolerance of the *aur* PKS toward Alternative Starter Units. A mutant lacking the *N*-oxygenase gene *aurF* is suitable for the mutasynthesis of aureothin derivative aureonitrile.[37] However, apart from cyanobenzoate we could not observe the incorporation of further alternative starter units. Surprisingly, the situation changed dramatically when we used another genetic construct in a different expression host. To generate deoxyaureothin derivatives, we deleted the *N*-oxygenase gene *aurF* as well as the cytochrome P450 monooxygenase gene *aurH* from the *aur* biosynthesis gene cluster. Both genes were subsequently excised from a cosmid bearing the entire *aur* locus by a combination of PCR-targeting and cloning strategies, respectively. The resulting plasmid, pMZ01, was introduced into the host strain *S. albus*, and the mutant strain was fermented in liquid production media. HPLC-MS monitoring of the extracts revealed that aureothin biosynthesis was fully abolished (Figure 3d). To complement the double knockout mutant, we supplemented the medium with PNBA and introduced a compatible expression plasmid (pMZ04), a pHJ110 derivative that contains the *aurF* gene downstream of the constitutive *ermE* promoter. Because these conditions fully restored aureothin biosynthesis, polar effects could be excluded. Using the Δ*aurFH* mutant supplemented with PNBA, we yielded 44.8 mg L^{-1} deoxyau-

(11) Menzella, H. G.; Reeves, C. D. *Curr. Opin. Microbiol.* **2007**, *10*, 238–245.
(12) Zhang, W.; Tang, Y. *J. Med. Chem.* **2008**, *51*, 2629–2633.
(13) Hertweck, C. *Angew. Chem., Int. Ed.* **2009**, *48*, 4688–4716.
(14) Khosla, C.; Keasling, J. D. *Nat. Rev Drug Discov.* **2003**, *2*, 1019–1025.
(15) Wilkinson, B.; Moss, S. J. *Curr. Opin. Drug. Discovery Dev.* **2005**, *8*, 748–756.
(16) Wilkinson, B.; Micklefield, J. *Nat. Chem. Biol.* **2007**, *3*, 379–386.
(17) Kirschning, A.; Taft, F.; Knobloch, T. *Org. Biomol. Chem.* **2007**, *5*, 3245–3259.
(18) Zhou, H.; Xie, X.; Tang, Y. *Curr. Opin. Biotechnol.* **2008**, *19*, 590–596.
(19) McGlacken, G. P.; Fairlamb, I. J. *Nat. Prod. Rep.* **2005**, *22*, 369–385.
(20) Wilk, W.; Waldmann, H.; Kaiser, M. *Bioorg. Med. Chem.* **2008**, *17*, 2304–2309.
(21) Busch, B.; Hertweck, C. *Phytochemistry* **2009**, *70*, 1833–1840.
(22) Hirata, Y.; Nakata, H.; Yamada, K.; Okuhara, K.; Naito, T. *Tetrahedron* **1961**, *14*, 252–274.
(23) Taginuchi, M.; Watanabe, M.; Nagai, K.; Suzumura, K. I.; Suzuki, K. I.; Tanaka, A. *J. Antibiot.* **2000**, *53*, 844–847.
(24) Cassinelli, G.; Grein, A.; Orezzi, P.; Pennella, P.; Sanfilippo, A. *Arch. Microbiol.* **1967**, *55*, 358.
(25) Takahashi, K.; Tsuda, E.; Kurosawa, K. *J. Antibiot.* **2001**, *54*, 548–553.
(26) Müller, M.; Kusebauch, B.; Liang, G.; Beaudry, C. M.; Trauner, D.; Hertweck, C. *Angew. Chem., Int. Ed.* **2006**, *45*, 7835–7838.
(27) He, J.; Hertweck, C. *Chem. Biol.* **2003**, *10*, 1225–1232.
(28) Traitcheva, N.; Jenke-Kodama, H.; He, J.; Dittmann, E.; Hertweck, C. *ChemBioChem* **2007**, *8*, 1841–1849.
(29) He, J.; Hertweck, C. *J. Am. Chem. Soc.* **2004**, *126*, 3694–3695.
(30) Winkler, R.; Hertweck, C. *Angew. Chem.* **2005**, *117*, 4152–4155.
(31) Winkler, R.; Richter, M.; Knüpfer, U.; Merten, D.; Hertweck, C. *Angew. Chem., Int. Ed.* **2006**, *45*, 8016–8018.
(32) He, J.; Hertweck, C. *ChemBioChem* **2005**, *6*, 908–912.
(33) Müller, M.; He, J.; Hertweck, C. *ChemBioChem* **2006**, *7*, 37–39.
(34) He, J.; Müller, M.; Hertweck, C. *J. Am. Chem. Soc.* **2004**, *126*, 16742–16743.
(35) Richter, M. E. A.; Traitcheva, N.; Knüpfer, U.; Hertweck, C. *Angew. Chem., Int. Ed.* **2008**, *47*, 8872–8875.
(36) Moore, B. S.; Hertweck, C. *Nat. Prod. Rep.* **2002**, *19*, 70–99.
(37) Ziehl, M.; He, J.; Dahse, H.-M.; Hertweck, C. *Angew. Chem., Int. Ed.* **2005**, *44*, 1202–1205.

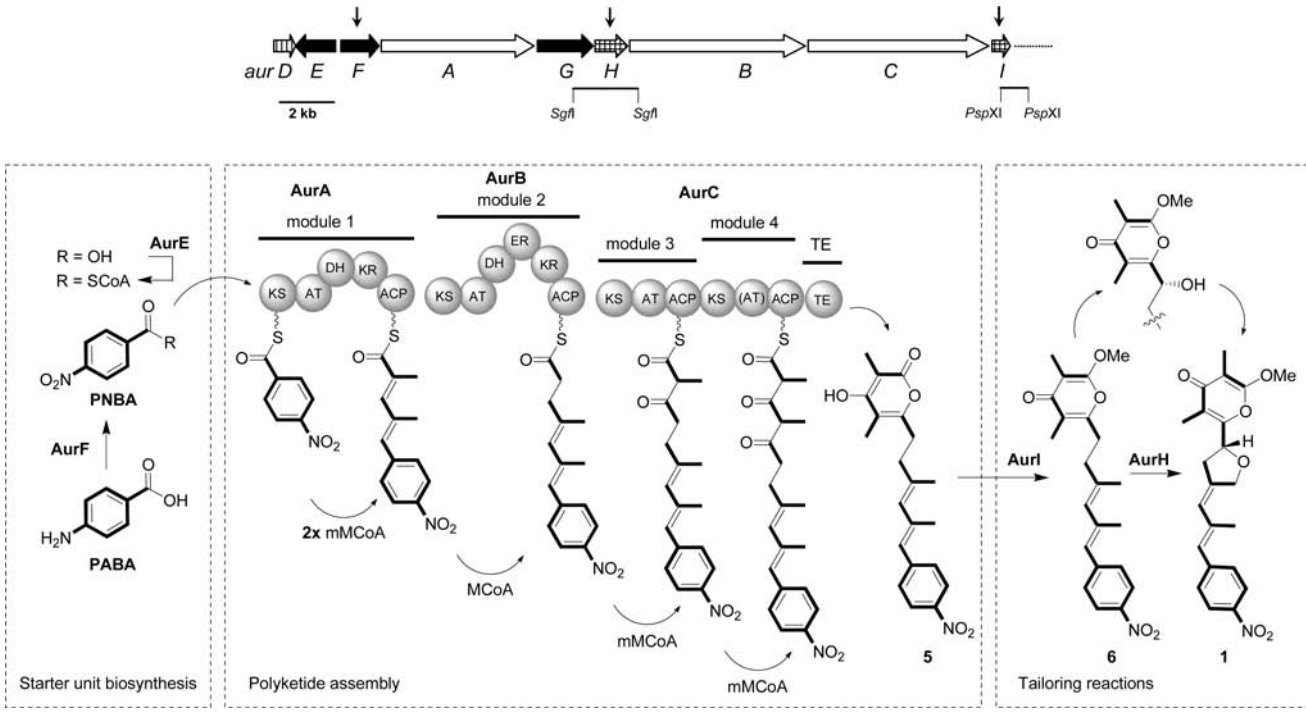

Figure 2. Organization of the *aur* biosynthesis gene cluster and model of the aureothin biosynthetic assembly line. AurG: PABA synthase, AurF: *N*-oxygenase, AurE: ligase, AurA-C: type I PKS, AurI: methyl transferase, AurH: Cyp450 monooxygenase.

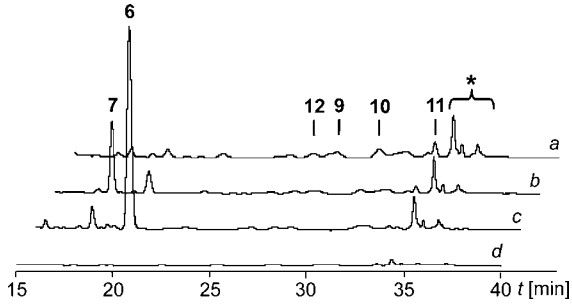

Figure 3. Metabolic profile of Δ*aurFH* null mutant (*S. albus*::pMZ01) supplemented with mixtures of mutasynthons (a) lacking PNBA (*p*-nitrobenzoate) and PCBA (*p*-cyanobenzoate), (b) lacking PNBA, (c) complete mixture, and (d) without supplement. (* indicates no relation to aureothin biosynthesis)

reothin on a 50 mL scale. This result encouraged probing starter unit surrogates. For testing the substrate tolerance of the PKS, the mutant *S. albus*::pMZ01 was supplemented with a series of substituted benzoates (BA, substitutions see below) in 25% aq DMSO ($c = 100\ \mu g\ mL^{-1}$) on a 50 mL scale. Initially, we tested the impact of chemical starter unit activation. For this purpose, we synthesized *N*-acetyl cysteamine (NAC) adducts that mimic CoA thioesters and readily diffuse into bacterial cells. However, when applying mutasynthons it proved to be irrelevant whether the analogues were supplied as SNAC thioester or as free acids. Apparently, the endogenous acyl-CoA ligase AurE is highly promiscuous and does not represent a bottleneck for engineering experiments.

The successful incorporation of the mutasynthons was monitored by HPLC and HRMS. The expected masses and isotope patterns were recorded for all deoxyaureothin derivatives (**7**−**11**) resulting from the incorporation of all *p*-halogenated BAs, and the pseudohalide *p*-cyanobenzoate. Likewise, we observed the incorporation of *p*-methyl-BA and *p*-methoxy-substituted benzoate, yielding **12** and **13**. It is remarkable that even benzoic acid is loaded onto the *aur* PKS and processed to a phenyl analogue of deoxyaureothin (**14**). The most surprising observation, however, was that even feeding 2-naphthoic acid yielded the corresponding pyrone (**15**). Another unexpected finding is that *m*-nitro-BA was tolerated as a surrogate, too, giving access to **16**. However, feeding alternative PNBA surrogates equipped with *ortho*- or *meta*-substituents or multiple functionalizations were not accepted as priming units. Likewise, no polyketide production was detected when supplementing the mutant with *p*-hydroxy-BA, *p*-amino-BA, *p*-*N*-methyl-amino-BA, *p*-*N*,*N*′-dimethyl-amino-BA or *p*-*N*-formamido-BA. Considering the tolerated substitutions, it appears that mutasynthons with electron-acceptor groups result in a higher production rate of the corresponding deoxyaureothin derivative than those with electron donor groups.

To evaluate the viability of a parallel biosynthesis of aureothin derivatives, we added mixtures of substituted benzoates to the Δ*aurFH* mutant (Figure 3a−c) and monitored the resulting metabolic profiles. Interestingly, mainly deoxyaureothin and deoxyaureonitrile are produced when adding the entire variety of possible starter units (Figure 3c). We next omitted PNBA and noted an increased production of deoxyaureonitrile (**7**) and several halogenated analogues (**8**−**11**) in low amounts (Figure 3b). Feeding a mixture lacking *p*-nitro-BA and *p*-cyano-BA led to a similar pattern but increased the yields of halogen- and methyl-substituted analogues (Figure 3a). These results clearly demonstrate the competition between the various possible starter units and that the formation of products derived from less-favored primers is repressed in the presence of *p*-nitro-BA and *p*-cyano-BA.

The *p*-cyanophenyl- and naphthoate-substituted derivatives were obtained from two fermentations in liquid R2YE media (20 L), yielding 2 mg L^{-1} of **7** and 1.8 mg L^{-1} of **15**, respectively. For the large scale production of *p*-halogenated derivatives, we selected liquid E1 medium, which proved to be

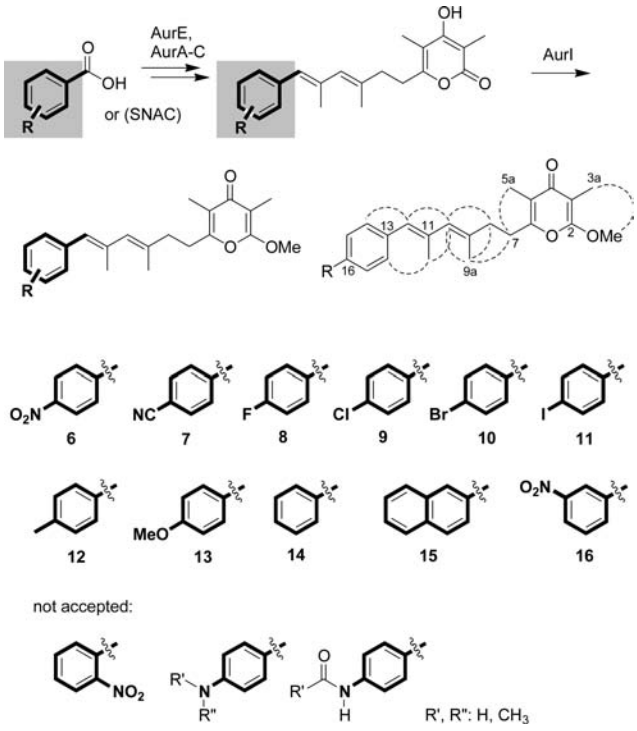

Figure 4. Structures of deoxyaureothin derivatives.

superior and less expensive, providing deoxyaureothin derivatives **8**−**11** in higher yields (R = F, 5.4 mg L^{-1}; R = Cl, 3.1 mg L^{-1}; R = Br, 7.8 mg L^{-1}; R = I, 18 mg L^{-1}). Taken together, we have shown that the *aur* PKS is rather promiscuous with regard to the starter units and that besides PNBA, ten different starter units can be employed for the preparative-scale precursor-directed biosynthesis of aureothin derivatives (Figure 4).

Exploiting Plasticity in Pyrone Formation through Mutational and Combinatorial Biosynthesis. At the pyrone moiety, three different substitution patterns (α-methylated, γ-methylated, and nonmethylated variants) are conceivable. For the production of nordeoxyaureothin derivatives, a triple mutant lacking *aurF*, *aurH*, and the *O*-methyltransferase gene *aurI* was constructed. This was achieved by a *Psp*XI restriction digest of cosmid pMZ01, which harbors a variant of the *aur* gene cluster lacking *aurF* and *aurH*. Because only two *Psp*XI sites are present in pMZ01, one within *aurI* and the other downstream of the *aur* locus, the target gene could be excised through restriction and religation. After verification of the correct construct, the resulting cosmid, pMZ02, was introduced into *S. albus* by conjugation. The exoconjugant *S. albus*::pMZ02 was tested at a 50 mL scale for the ability to produce desmethylated analogues. Although no polyketide production was observed for the mutant in liquid R2YE complex medium, supplementation with PNBA yielded nordeoxyaureothin (**5**), which features the more stable nonmethylated α-pyrone ring.

PNBA surrogates were analogously accepted by the triple mutant, yielding analogues such as nordeoxyaureonitrile (**7**) with different aryl substitutions. Complementation of the triple mutant with *aurI* restored the formation of the methylated γ-pyrone.

To expand the scope of substitutions, we aimed at generating an *O*-metylated α-pyrone. As yet, the only known enzyme catalyzing an *O*-methyl transfer of a pyrone metabolite is EncK from the enterocin pathway in *Streptomyces maritimus*.[38,39] To test whether this enzyme has a sufficiently broad specificity to

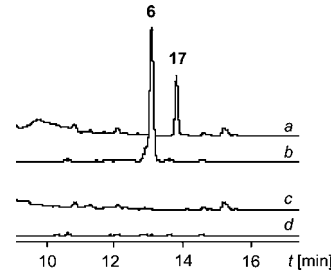

Figure 5. Regiospecific pyrone *O*-methylation by AurI and EncK. HPLC profiles of extracts from (a) Δ*aurFHI* triple mutant (*S. albus*::pMZ02), complemented with *encK* (*S. albus*::pMZ02/pHJ72) supplemented with PNBA, (b) Δ*aurFH* mutant (*S. albus*::pMZ01) supplemented with PNBA, and (c) *S. albus*::pMZ02/pHJ72, d) *S. albus*::pMZ01.

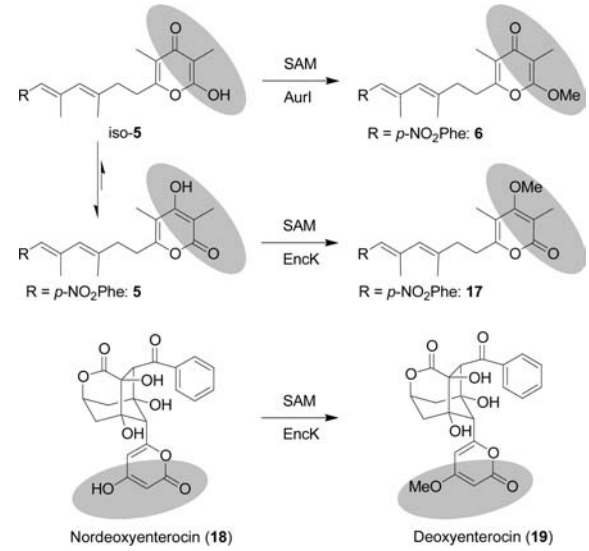

Figure 6. Regiospecific pyrone *O*-methylation by AurI and EncK.

methylate the aureothin pyrone ring, we planned to complement the Δ*aurFHI* null mutant with *encK*. For this purpose, *encK* was recovered from cosmid 1A9 as 1.8 kb *Eco*RI fragment and cloned downstream of the constitutive *ermE* promoter of pWHM4*. The resulting construct, pHJ72, was introduced together with pMZ02 into *S. albus*. The resulting strain (*S. albus*::pMZ02/pHJ72) was cultured with apramycin and thiostreptone as selection markers, and its metabolic profile was monitored by HPLC/MS. In fact, supplementation of the mutant with PNBA yielded a new product (**17**). While **6** and **17** share the same molecular mass, they have a markedly different retention time in the HPLC profile, thus suggesting they represent two regioisomers (Figure 5). This was firmly corroborated by NMR data. The successful methylation of **5** using EncK is surprising in light of the different polyketide core structures of aureothin and enterocin (Figure 6). Notably, only *encK* can complement the Δ*aurI* mutant and not vice versa (data not shown), indicating that EncK has broader substrate specificity than AurI. In sum, the Δ*aurFHI* mutant allows access to aureothin derivatives with modified pyrone moieties. Upon supplementation with PNBA or other synthetic analogues, it is possible to yield various homologues.

(38) Piel, J.; Hertweck, C.; Shipley, P.; Hunt, D. S.; Newman, M. S.; Moore, B. S. *Chem. Biol.* **2000**, *7*, 943–955.
(39) Cheng, Q.; Xiang, L.; Izumikawa, M.; Meluzzi, D.; Moore, B. S. *Nat. Chem. Biol.* **2007**, *3*, 557–558.

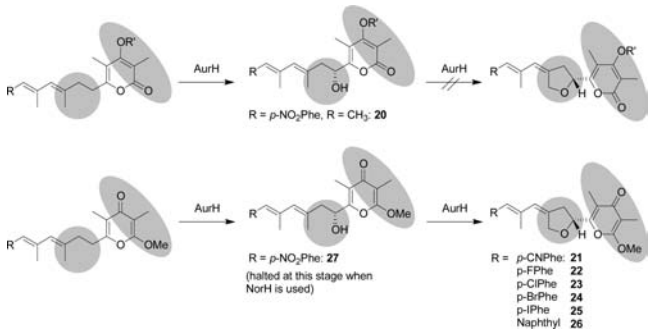

Figure 7. Biotransformation of α- and γ-pyrones by AurH.

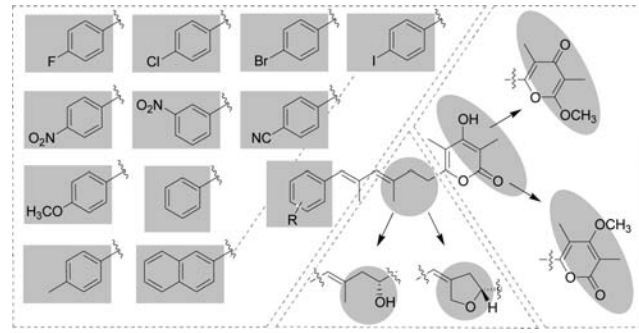

Figure 8. Survey of conceivable aureothin derivatives.

Promiscuity of the Bifunctional Monooxygenase AurH in Polyketide Hydroxylation and Heterocyclization. The sequential, AurH-catalyzed hydroxylation−heterocyclization represents the last step in the aureothin pathway. From initial mutasynthesis experiments using the Δ*aurF* mutant, it appeared that various aureothin derivatives are toxic for the producer strain, thus limiting their continuous formation. For this reason, we chose to generate aureothin derivatives containing the characteristic chiral tetrahydrofuran moiety by AurH-mediated biotransformation of the deoxyaureothin derivatives. While the in vitro biotransformation with AurH is in principle viable,[35] an in vivo approach using whole cells of a host expressing *aurH*[40] proved to be more efficient on the preparative scale. For this purpose, the aureothin cytochrome P450 monooxygenase AurH was heterologously expressed in *S. albus* and *S. lividans* using expression plasmid pHJ110. HPLC-MS monitoring of 50 mL cultures of *S. lividans*/pHJ110 supplemented with deoxyaureothin derivatives indicated in all cases the formation of novel peaks with complete disappearance of the starting material (Figure 7). AurH proved to be remarkably tolerant toward artificial substrates. The oxygenase is capable of transforming deoxyaureonitrile (**7**), all four *p*-halogenated derivatives (**8**-**11**), and even the unusual naphthoate (**15**) into the corresponding aureothin analogues **21**-**26**. However, when α-pyrones like **17** were administered, no heterocycle formation was observed. Instead, 7-hydroxy derivatives such as **20** were produced. *O*-Heterocyclization obviously only takes place in the presence of a methylated γ-pyrone moiety, where an exact enzyme fit is warranted. If desired, it would also be possible to introduce a 7-hydroxyl moiety into methylated γ-pyrones and circumvent THF ring formation. This is generally feasible when complementing the *aurH* null mutant with *norH* from the neoaureothin pathway, since NorH is not capable of catalyzing the full reaction sequence when an aureothin backbone is supplied. In this way, appreciable amounts of the 7-hydroxylated γ-pyrone **27** were obtained.

The scale-up for preparative in vivo biotransformations was optimized using *p*-iododeoxyaureothin (**11**) dissolved in DMSO (6.5 μmol, c = 1 mg 25 μL^{-1}) in 250 mL M10 media. As a result of its reduced metabolic background *S. albus*/pHJ110 proved to be superior to *S. lividans*. Varying amounts of **11** (6.5, 13, c. 26, and 52 μmol) were tested, revealing an optimum of production when using the lowest quantity of the corresponding aureothin analogue **25** (74%, 52%, 52%, 40%, respectively) as quantified by HPLC.

Production of a Focused Library of Aureothin Derivatives by Fermentation. The mutasynthesis experiments revealed that at least 11 different starter units are accepted by the aureothin PKS. Furthermore, three modes of backbone substitutions and three different types of pyrone moieties can be engineered through biotransformation and combinatorial biosynthesis, respectively (Figure 8). The only restriction is that the tetrahydrofuran ring is not readily formed in the presence of α-pyrones. Accordingly, at least in principle, 77 aureothin derivatives would be accessible through the combination of all methods presented. However, not all compounds appeared to be equally profitable; we found that nonmethylated α-pyrones and hydroxyl-substituted aureothin analogues (e.g., **20**, **27**) are prone to acid-catalyzed degradation and rearrangement, which renders them less favorable from a pharmacological point of view. Furthermore, initial biological assays indicated that a deoxyaureothin derivative featuring an α-pyrone (**17**) moiety exhibit a markedly lower antiproliferative effect (Huvec GI_{50} >20 $\mu g\ mL^{-1}$) compared to the γ-pyrone **6** (Huvec GI_{50} 9.3 $\mu g\ mL^{-1}$). Furthermore, the α-pyrone proved to be slightly more cytotoxic, which is against the desired disposition. In addition, the methylated α-pyrone compounds do not show any antifungal activity (Figure 10). We thus focused on the large scale production of all *p*-cyano-, *p*-halogen-, and naphthoate-substituted deoxyaureothin (**7**−**11**, **14**, **15**) and aureothin derivatives (**22**−**26**) featuring the methylated γ-pyrone group. The α-pyrone **17** and the 7-hydroxy substituted analogues **20** and **27** were also produced on a preparative scale for comparison.

The mutasynthesis experiments for the production of the methylated γ-pyrones were performed by multiple 20 or 60 L fermentations. The culture broths were neutralized with 1 N HCl, and mycelia and culture filtrates were individually extracted with ethyl acetate. Crude extracts were subjected to open column chromatography (silica gel, normal phase) using a $CHCl_3$/MeOH gradient. Final purification was achieved by preparative reverse phase HPLC. For subsequent biotransformations, the deoxyaureothin derivatives were transformed into the corresponding aureothin derivatives using AurH in a whole cell approach as described above, yielding 74% conversion.

It should be highlighted that the structures of all new compounds (**7**−**11**, **14**, **15**, **17**, **20**, **22**−**27**) were fully elucidated by 1D and 2D NMR experiments, high resolution mass spectrometry, and infrared spectroscopy. NMR shifts of the core structures were similar to those of **1** and **6**, respectively. The influence of the groups exerting different I- and M-effects was clearly detected in shifts of the neighboring atoms. Signals of the fluoro-substituted analogues showed typical C−F coupling constants (ranging from 259 to 3 Hz) up to 6 atom bondings in the ^{13}C NMR. Two-dimensional NMR as well as NOESY experiments fully support the proposed structures. HR-MS data confirmed the expected molecular masses, and chloro- and

(40) Werneburg, M.; Hertweck, C. *ChemBioChem* **2008**, *9*, 2064–2066.

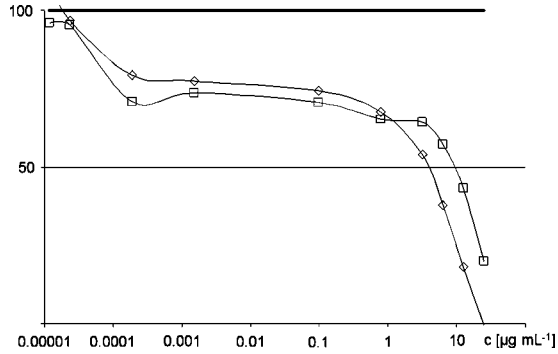

Figure 9. Antiproliferative effects of *p*-fluoro-aureothin (□, **22**) and *p*-fluoro-deoxyaureothin (◇, **8**) on human K-562 leukemia cells displayed in a dose−response curve; concentration vs proliferation (% vs control, bold line).

bromo-derivatives showed the typical isotopic pattern ("A + 2") in the mass spectra. By IR-spectroscopy the vibration of the nitrile group as well as the C−Hal vibrations could be clearly observed. The IR fingerprint (ca. 850−810 cm^{-1}) indicated the *para*-substitution of the phenyl headgroup.

Identification of Novel Aureothin Derivatives with Selective Antifungal and Improved Antiproliferative Activities. The biological activities of all new aureothin derivatives were analyzed in a panel of assays with the cell lines human cervix carcinoma HeLa, mouse fibroblast cells L-929, human umbilical vein endothelial cells Huvec, as well as human K-562 leukemia cells. Notably, almost all new compounds show increased antiproliferative and cytostatic activities compared to those of aureothin (**1**) and have significantly lower cytotoxicity. For deoxyaureonitrile (**7**) and the halogenated deoxyaureothin derivatives (**8**−**11**) a dramatic increase in antiproliferative activities (up to 50-fold compared to **1**) could be determined, with GI_{50} values (K-562) as low as 0.5 $\mu g\ mL^{-1}$. Furthermore, the antiproliferative compounds show intriguing dose−response curves with a plateau over several orders of magnitude (Figure 9). Such a flat curve is favorable considering a broad therapeutic window. A combination of both a flat curve and low IC_{50} values may be beneficial for potential therapeutic applications.

The most remarkable finding in our biological assays was the selective antifungal activity of the new aureothin derivatives. Using a panel of bacteria, yeasts and fungi (Figure 10), the novel aureothin derivatives were compared to the known substances deoxyaureothin (**6**), aureothin (**1**) and aureonitrile (**21**). Except for deoxyaureonitrile (**7**), deoxyaureothin analogues do not show any notable antibacterial activities. Compared to deoxyaureothin (**6**), deoxyaureonitrile (**7**) exhibits a higher activity against *Sporobolomyces salmonicolor* and *Penicillium notatum*. In contrast, the new aureothin derivatives **22**−**25** show activities similar to those of **1** and **21** against these test strains as well as the important pathogen *Candida albicans.* Because of the remarkable activity of various aureothin derivatives against the yeast *Sporobolomyces salmonicolor*, the facultative human pathogen *Candida albicans*, and the mold *Penicillium notatum*, an extended array of fungal test strains including human pathogenic *Aspergillus* spp. was probed. Deoxyaureonitrile (**7**) shows selective antifungal activity against *Aspergillus niger* and *Aspergillus fumigatus*, the major cause for human aspergillosis. Compounds **22**−**25** are even more active against aspergilli, in particular the pathogen *Aspergillus terreus*. Although **22** and **24** do not show any activity against *Candida glabrata*, they effectively inhibit the growth of *Glomerella cingulata*, the

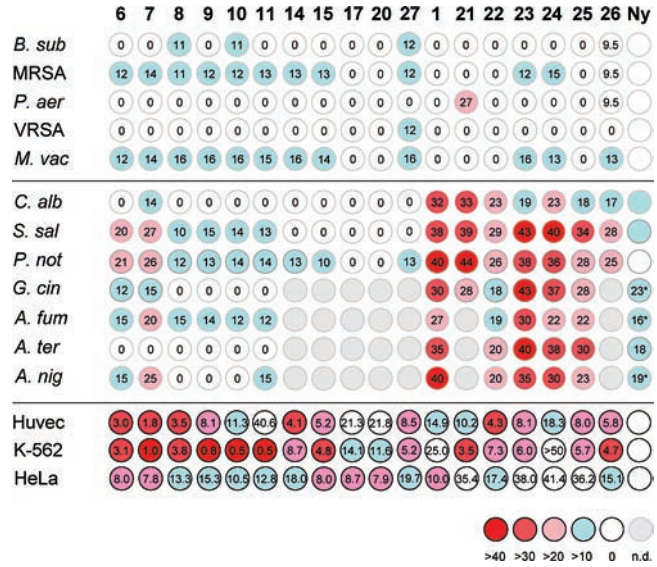

Figure 10. Color-coded survey on antimicrobial (inhibition diameter in mm), cytotoxic ($IC_{50}\ \mu g\ mL^{-1}$) and antiproliferative ($GI_{50}\ \mu g\ mL^{-1}$) activities of aureothin (**1**) and its derivatives. Less effective activities indicated with blue and color-staggered to dark red for the most effective ones. Test strains: *Bacillus subtilis* ATCC 6633; *Staphylococcus aureus* SG511; *Pseudomonas aeruginosa* K799/61; *Enterococcus faecalis* (VRSA) 1528; *Mycobacterium vaccae* 10670; *Candida albicans* BMSY 212; *Sporobolomyces salmonicolor* 549; *Penicillium notatum* JP36; *Glomerella cingulata*; *Aspergillus fumigatus* ATCC 46645; *Aspergillus terreus* DSM 826; *Aspergillus niger* DSM 737. Ny: nystatin.

phytopathogenic fungus and causative agent of apple bitter rot. Among all tested compounds, *p*-chloroaureothin **23** proved to be the most active antifungal agent.

Comparing the activity profiles of deoxyaureothin and aureothin derivatives, it is obvious that the presence of the tetrahydrofuran unit is critical for the antifungal activity, in particular against yeasts. It should be highlighted that **22** and **24** are significantly more active against *Aspergillus fumigatus*, *Aspergillus terreus* and *Aspergillus niger* than the standard references nystatin and amphotericin B (not shown). The selective activities against fungal strains are striking.

Conclusion

Aureothin is a densely functionalized natural product with intriguing biological activities, yet toxic and pharmacologically unfavorable due to the nitroaryl substitutent. The aim of our study was to generate a series of aureothin analogues for structure−activity relationship (SAR) studies. Because of the relatively small size of both molecule and the corresponding biosynthesis gene cluster, this target was ideally suited as a model for combining genetic, biochemical, and chemical methods to generate structural diversity. Furthermore, the aureothin pathway exhibits three principal levels that could be envisaged for diversification: the aryl starter unit, the oxygenated backbone, and the pyrone headgroup. To efficiently replace the nitro substituent, we chose the concept of bioisosterism that is well-known in drug design.[41] This goal was achieved through mutasynthesis using an engineered Δ*aurF/aurH* null mutant that exhibits a broad substrate tolerance toward 10 alternative PKS starter units. Furthermore, in a combinatorial biosynthesis approach, we found that the endogenous γ-regiospecific pyrone methyltransferase (AurI) can be replaced by an α-regiospecific

(41) Lima, L. M. A.; Barreiro, E. J. *Curr. Med. Chem.* **2005**, *12*, 23–49.

homologue from the enterocin pathway (EncK), yielding the corresponding iso-deoxyaureothin derivatives. Finally, the aureothin cytochrome P450 monooxygenase, AurH, was used as a tool for whole cell enzymatic hydroxylation and heterocyclization, repectively, providing a convenient access to the chiral tetrahydrofuran moiety. By this highly integrative approach in total 15 aureothin analogues were generated on a preparative scale. A biological evaluation of these compounds revealed new insights into structure−activity relationships and identified various promising candidates. Some of the new deoxyaureothin derivatives are less cytotoxic but stronger antiproliferative agents than the parent natural product. Furthermore, some of the new aureothin derivatives hold promise as highly selective antifungals, in particular anti-*Candida*, and it seems that the THF ring markedly increases antifungal activity. Our results demonstrate that exploiting enzymatic promiscuity may well complement synthetic approaches to generate structural diversity. Thus, our results are another illustration for the viability and potential of biosynthetic engineering.

Acknowledgment. This work has been financially supported by the DFG within the framework of SPP1152 and the NIH (AI47818). We thank C. Heiden and M. Steinacker for performing fermentation and downstream processings, U. Wohlfeld and M. G. Schwinger for antimicrobial assays, and E.-M. Neumann for antiproliferative and cytotoxic assays, and A. Perner and F. A. Gollmick are acknowledged for MS and NMR measurements, respectively.

Supporting Information Available: Experimental details, physicochemical data, biological assays, and NMR spectra. This material is available free of charge via the Internet at http://pubs.acs.org.

JA102751H